SCIENCE CHINA
Earth Sciences

• RESEARCH PAPER •

August 2010 Vol.53 No.8: 1216–1228
doi: 10.1007/s11430-010-3040-1

Monitoring the 2008 cold surge and frozen disasters snowstorm in South China based on regional ATOVS data assimilation

LU QiFeng[1], ZHANG WenJiang[2,3*], ZHANG Peng[1], WU XueBao[1], ZHANG FengYing[1], LIU ZhiQuan[1,4] & DALE M. Barker[4]

[1] *Key Laboratory of Radiometric Calibration and Validation for Environmental Satellites, China Meteorological Administration, National Satellite Meteorological Center, Beijing 100081, China;*
[2] *Institute of Geographic Sciences and Natural Resources Research, Chinese Academy of Sciences, Beijing 100101, China;*
[3] *State Key Laboratory of Hydraulics and Mountain River Engineering, Sichuan University, Chengdu 610065, China;*
[4] *National Center for Atmospheric Research, Boulder, Colorado, USA*

Received March 26, 2009; accepted November 6, 2009; published online May 15, 2010

In January 2008, South China experienced extremely low temperatures, heavy snowstorms, and severe frosts (2008 Frost Disaster, for short), which led to (partial) failures of observations from ground stations and ground radars resulting in a lack of necessary emergency information. To compensate for the failure of ground observations and to provide timely disaster information, the National Satellite Meteorological Center of China (NSMC) established a snow storm monitoring system for the 2008 Frost Disaster, which was based on the WRF Three Dimension Variational Assimilation and Forecast system (with NOAH as the land surface sub-process model) cooperatively developed by NSMC and the National Center for Atmospheric Research (NCAR), US. This system made full use of ATOVS and NCEP data to provide estimates of snow water equivalent every 6 hours during the storm. In this study, the ATOVS assimilation based snowstorm monitoring scheme was explored in detail, while the modeled results with and without ATOVS assimilation were compared against related observations. Results showed that the coupling of ATOVS assimilation into the proposed monitoring system evidently delineates weather characteristics of the snowstorm process more accurately, and demonstrated the feasibility of the system for snowstorm monitoring and forecasting. Through theoretical analyses and case discussion, this study proposes a reliable and practicable scheme to provide timely and accurate information on snow spatial distribution and temporal development for disaster mitigation, and illustrates a new application of ATOVS data.

2008 cold surge and frozen disaster in South China, ATOVS data assimilation, snow depth, snowstorm monitoring

Citation: Lu Q F, Zhang W J, Zhang P, et al. Monitoring the 2008 cold surge and frozen disasters snowstorm in South China based on regional ATOVS data assimilation. Sci China Earth Sci, 2010, 53: 1216–1228, doi: 10.1007/s11430-010-3040-1

In China, snowstorms occur mostly in its Northeast and Northwest regions and in its Tibetan Plateau [1], where many studies [2–5] have been carried out to understand more completely the synoptic mechanisms triggering snow storms. Such studies have improved monitoring, early warning, and handling of such disasters in these regions. In middle and late January of 2008, South China experienced a rare and severe cold surge that produced extremely damaging frosts, snow, and ice storms. Prolonged, heavy precipitation occurred over an extensive area of South China. Because of the lack of experience in this region in the monitoring, early-warning, and quick response to such disasters, the event severely impacted daily life and productivity, by seriously damaging transportation, communication, electric-

*Corresponding author (email: zhangwj@lreis.ac.cn)

ity, and other essential services [6]. In such events, spatial distribution and, especially, snow depth are the most critical characteristics directly affecting daily life. When snow depth reaches a certain threshold, it is likely to threaten transportation, communication, electricity, structures, agriculture, forests, etc. Accurate snow information in real-time is therefore required to correctly evaluate such a disaster, and allow efficient, effective, and rapid response.

Conventional ground observations, radar echo observations, and satellite remote observations have been widely used to monitor major snowstorms. Ground observations are the most accurate and direct way to measure and provide snow depth information [7]. Echo-related data from Doppler radar provides detailed snowfall information on features such as water vapor, low level jet and cloud structure. More accurate snow information could be retrieved by determining the mathematical and physical relationship between snow parameters and radar echo [8–10]. For periods with clear sky, snow depth information could be retrieved by empirical models derived from remote observations using satellites' visible and infrared channels [11, 12]. Microwave imagers can generate quantitative snow depth information [13–17]. Retrieval of snow depth and snow water equivalents by the U.S. is based on SMMR (Scanning Microwave Multi-band Radiometer) and SSMI (Special Sensor Microwave/Imager) observations.

In January of 2008, however, available observations were insufficient to monitor the snowstorm, due to the partial failure of surface instruments caused by the extremely low temperatures over a prolonged period coupled with persistent cloud cover. No sufficiently comprehensive and efficient observational data could be collected in time. Some radar receiver antennas were covered by snow, causing some emitters to fail and forcing data outages. Satellite visible and infrared observations failed to provide snow depth information due to heavy cloud contamination, while the U.S. SMMR and SSM/I data, capable of penetrating clouds, were not available in time during the disaster period.

It is widely agreed that the occurrence of snowstorms is always closely related to atmospheric circulation of large scale circulation [2, 18–22]. Numerical Weather Prediction models (NWP) can forecast spatially and temporally continuous circulation at a large scale, but their accuracy is dependent on initial conditions. Snow information could be further derived by NWP models through a coupled land surface sub-model (capable of delineating snow physics). Two key questions here therefore are: could more accurate atmospheric circulation information be simulated by using more accurate initial conditions; and could snow information with increased accuracy be retrieved by the snow parameterization scheme in a land surface sub-model?

A major goal of this study is to answer these two questions. To do this, two requirements must be met: to provide more accurate initialization information for the NWP models and to deduce snow information from accurate near-surface parameters and a reliable snow physical parameterization scheme. Initialization fields with higher accuracy could be obtained by assimilating more observations into an NWP model. In particular, the assimilation of ATOVS (Advanced TIROS Operational Vertical Sounder) data brings significant improvements in atmospheric circulation prediction [23–25], which could further produce more accurate near-surface parameters. The snow-related processes of falling, accumulation, sublimation and thawing, and the heat exchange at both snow-atmosphere and snow-soil interfaces all could be simulated by coupling a snow physical model into the land surface sub-model [26, 27]. The snow information necessary for monitoring snowstorms could be further analyzed, which could provide information on snow depth and its spatial-temporal distribution with increased accuracy based on more reliable near-surface parameters and the snow parameterization procedure.

The ATOVS data[1)] received and preprocessed by NSMC contain not only information on large scale atmospheric circulation but also local surface information available in real time [28]. NSMC has cooperated with NCAR to develop the WRF (Weather Research and Forecast) assimilation/forecast system into which the ATOVS data, received and preprocessed by NSMC, could be assimilated and the snow physics processes could be simulated better by the NWP model's snow parameterization scheme.

In order to provide high-spatial resolution snow information for the 2008 Frost Disaster monitoring service, a snowstorm monitoring system was established. It is based on regional ATOVS satellite observations, NCEP (National Center for Environmental Prediction) data and the WRF three dimensional variational (3D-Var, for short) assimilation and forecast system. The NOAH land surface model was selected to accurately delineate the snow physics. The assimilation of ATOVS observations into the snowstorm monitoring system generated more accurate near-surface parameters, by which the parameterized snow physics scheme in the NOAH[2)] land surface model [29] could be driven to produce more accurate snow information for snowstorm monitoring. The evolution of snow water equivalent every 6 hours during the 2008 Frost Disaster was diagnosed, which helped monitor the disaster and supplied efficient and near real-time snow information for the weather diagnosis meetings.

1) ATOVS data include the High-resolution Infrared Radiation Sounder (HIRS), the Advanced Microwave Sounding Unit-A (AMSU-A) and the Advanced Microwave Sounding Unit-B (AMSU-B) or Microwave Humidity Sounder (MHS) to detect vertical atmosphere structure.

2) NOAH initially was composed of four participants; N, National Centers for Environmental Prediction; O, Oregon State University; A. U.S. Air Force; H, Hydrologic Research Lab-NWS.

1 Designing the snowstorm monitoring scheme based on ATOVS data assimilation and assessing its feasibility

The forecast and assimilation system adopted for the regional satellite ATOVS data assimilation was jointly developed by NCAR and NSMC, based on the WRF 3D-Var assimilation/forecast systems. It contains two components: the forecast system and the satellite ATOVS data assimilation system. The ability to assimilate regional satellite ATOVS data is a new feature of the WRF 3D-VAR developed by the authors' group.

1.1 Forecast system

The forecast system used in this study is the Weather Research and Forecasting (WRF) Model, jointly developed by the researchers [30, 31] from the U.S. government and university institutes. Its software architecture permits parallel computation and system extendibility, which integrates all the newest achievements [32] in the field of meso-scale meteorology. It especially focuses on meso-scale weather forecasting from clouds to the weather scale of 1–10 km. It replaces the MM5 model.

1.2 ATOVS data assimilation system

The adopted assimilation system for the regional satellite ATOVS data was jointly developed by NCAR and NSMC based on the WRF 3DVAR scheme to assimilate the ATOVS data. The ATOVS data assimilation system includes four modules: assimilation frame, fast radiation transfer model, data quality control, and radiation bias correction.

1.2.1 Assimilation system frame

The assimilation system frame is the major component to optimally minimize the dynamic model and the observations provided. The WRF 3D-Var assimilation system [33] was developed based on the MM5 3D-Var assimilation system [34], and the cost function is solved using the conjugate gradient and quasi-Newtonian descending methods following Lorenc's suggestion [35].

1.2.2 Observation operator

The observation operator is a fast radiative transfer model (RTM), which converts model state variables into observation space. In contrast to data assimilation of conventional observations, the observation operator for satellite data assimilation is a complex RTM. To assimilate TOVS/ATOVS data, the ECMWF (European Centre for Medium-range Weather Forecasts) first developed a fast RTM, RTTOV [36], which permits direct assimilation of satellite radiance data. With updates of ATOVS instruments, RTTOV was also updated periodically, and RTTOV version 8.7 was used in this study. With the cooperation of NSMC and NCAR, the regional ATOVS data were assimilated into the WRF 3D-Var system with RTTOV as the observation operator [37].

1.2.3 Data quality control

A data quality control module determines which data go into the assimilation system, which has direct influence on the analysis. Therefore, the data quality control module is crucially important for satellite data assimilation systems. Data quality control was performed in two steps. First, a crude check was made based on the simulated and the observed brightness temperature. The decision rule used was that the data will be used, if $150 < Tb_{\text{obs}} < 350$ and $(Tb_{\text{obs}}-Tb_{\text{fg}}) < 15$, and $(Tb_{\text{obs}}-Tb_{\text{fg}})^2 < (O^2+B^2)$, where Tb_{obs} and Tb_{fg} stand for observed and simulated brightness temperature, respectively, and O and B for observation error and background field error. For the second step, a more careful check was done for different channels. To select the satellite data to use in the assimilation system, e.g., HIRS (20 channels), AMSUA (15 channels), and MHS (5 channels), channel composition information was used to check data quality. However, if the difference between simulated and observed brightness temperatures was large, then a further determination of data quality was used: if $|Tb_{\text{obs}}-Tb_{\text{fg}}| > 3\times|O|$, the observed data were rejected.

1.2.4 Radiation bias correction

The bias correction module mainly corrects the systematic bias caused by the inaccuracy of the observation operator. The Harris and Kelly method [38] was used to correct the radiation bias in the assimilation system, and also followed Eyre's method [39], i.e., by first calculating the scan-dependent correction and then an airmass-dependent correction for the residual. The scan-dependent correction is calculated individually for 10° latitude bands. Northernmost and southernmost bands are broadened to give a reasonable capture of data and the correction is then smoothed between latitude bands to give a smooth transition across the band boundaries. The residual, i.e., the airmass-dependent bias, is modeled as a function of the following predictors taken from the NWP model background: 1000–300 hPa thickness, 200–50 hPa thickness, surface skin temperature (SST), and total column water vapor.

1.3 Feasibility analysis of snowstorm monitoring scheme based on ATOVS data assimilation

Figure 1 shows the relationship of observed snow depth over the snowstorm region and the brightness temperature observed with channel 5 of the NOAA18/ATOVS MHS at 06 UTC (06:00 UTC, the same below) of 28 January 2008, with a weighting function at 700 hPa indicating the water vapor transfer feature. Figure 1 also shows a cold zone ranging southwestwardly from the Yungui (Yunnan and

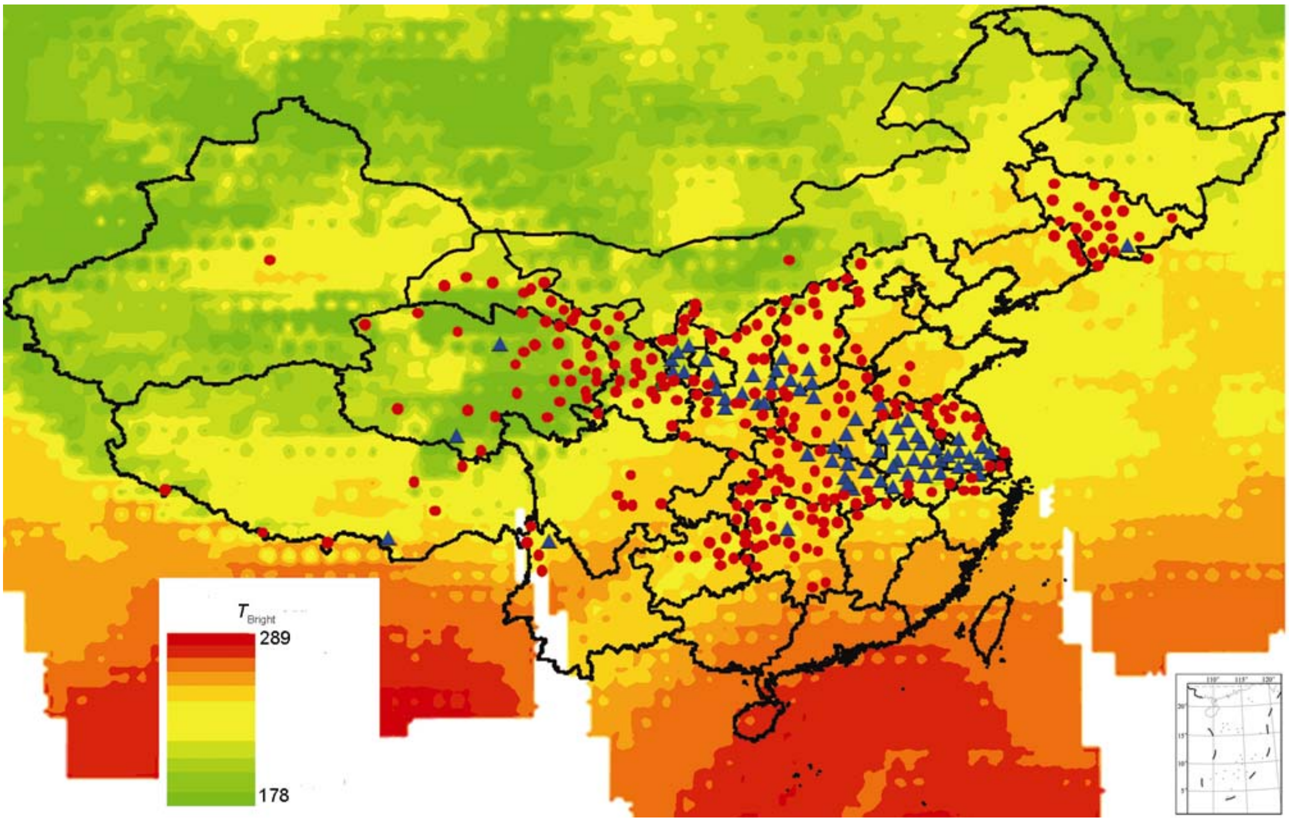

Figure 1 Observed snow depth and brightness temperature at channel 5 of NOAA18/ATOVS MHS on 06 UTC 28 January 2008. Blue triangles and red dots are stations with snow depth more than or less than 12 cm, respectively.

Guizhou) Region to the Yangtze-Huaihe Region, which corresponds to the water vapor transportation zone at 700 hPa from the Indian Ocean to Bay of Bengal. The cold area in the background of observed brightness temperature agreed well with the observed area of heavy snowfall, while lower brightness temperature over the Yangtze-Huaihe Region corresponded to more heavy snowfall. Meanwhile, the brightness temperature decreased extensively over a large area, caused by cold air invasion current from Siberia into China, and coincides with the actually observed heavy snowfall over the region.

Comparison of brightness temperature in channel 5 of NOAA18/ATOVS MHS and snow depth observation showed good agreement and therefore indicated that information on temperature decrease and snowfall can be deduced from the satellite-observed ATOVS data.

1.4 Design and verification of the regional ATOVS data assimilation experiment

Snowstorms are often closely related to large scale circulation events, but surface atmospheric state parameters drive several important snow physics evolution processes, such as snow-atmosphere radiative transfer, the hydrological processes in the snow (snow freezing, melting, evaporation, sublimation, and snow water transfer intra soil) and the sensible/latent heat fluxes at snow-atmosphere and snow-soil interfaces, etc. Therefore, with the given snow parameterization scheme, the accuracy of these surface atmospheric parameters will directly determine the accuracy of modeled snow parameters. The ATOVS assimilation system absorbs the ATOVS brightness temperature information into state variables. After ATOVS assimilation, a more accurate atmospheric circulation can be expected, with improved simulation of variables in every atmospheric layer and near the surface. Furthermore, accurate snow depth and snow water equivalent information could be derived by selecting the NOAH land surface sub-model in the WRF forecast model to delineate snow accumulation, sublimation, melting, and heat exchange at the snow-atmosphere and snow-soil interfaces.

1.4.1 Design of assimilation experiment

The objective in this study was to obtain high-resolution snow information (30 km×30 km) for the emergency services during the South China snowstorm disaster by assimilating regional ATOVS data and using the snow monitoring scheme described above. To this end, the experiment's regional center is set at the location, 115°E, 30°N, in the area southeast to Wuhan, which is located in the southeastern China, with a 30 km horizontal resolution and a 28 layer vertical resolution. The experiment is driven by NCEP forecast fields and uses the following physical procedures: Mellor-Yamada-Janjic TKE Boundary Layer scheme, NOAH land surface model, Monin-Obukhov similarity scheme, Betts-Miller-Janjic cloud convection scheme, NCEP micro-physics scheme, RRTM long-wave radiation scheme, and the Dudhia short wave radiation scheme. The assimilation experiment is performed with 6-hour assimilation windows at 00, 06, 12, and 18 UTC (corresponding to 21–03, 03–09, 09–15, and 15–21 UTC), and was post-processed by NCAR-GRADS software.

1.4.2 Verification of the assimilation scheme

To verify the feasibility of the regional ATOVS data assimilation scheme, the geo-potential height at 500 hPa from ECMWF and meteorological elements of typical observation stations from CMA were used to examine the effects of ATOVS assimilation.

1) Comparison of geo-potential height fields. Figure 2 presents information on geo-potential height with and without ATOVS assimilation on 06 UTC 28 Jan 2008. Figure 2 shows that the 540 contour line over Barekashi Lake of Kazakhstan and over Xinjiang in northwestern China was simulated more accurately with ATOVS assimilation. Also, the region with rich snowfall is evident in the difference chart of the initial field with and without ATOVS assimilation. This indicates that ATOVS data influences the data assimilation system.

2) Verification based on single station observations. The joint interaction of the Ural blocking high, the cold airflow from the north to the south, and the trough forming a water vapor jet transport belt in South China caused the prolonged cold surge and the severe frost disaster in South China. The geo-potential height and temperature at 500 hPa could closely reflect the Ural blocking high feature and the cold airflow from north to south. The wind field and water vapor at 700 hPa are the key factors in forming and maintaining the water vapor jet transport belt. The accuracy of these four elements determines the ability to correctly simulate the circulation pattern that caused the snowstorm disaster. Consequently, the temperature and geo-potential height at 500 hPa and humidity and the wind fields at 700 hPa were selected to verify the influence of the assimilation.

Guizhou was one of the regions most heavily damaged by the Disaster, so the meteorological observations at Guiyang station (106.73°E, 26.58°N) were selected for verification. In Figure 3, the simulated temperature, humidity, geo-potential height, and wind vector field at Guiyang station with and without ATOVS assimilation were compared

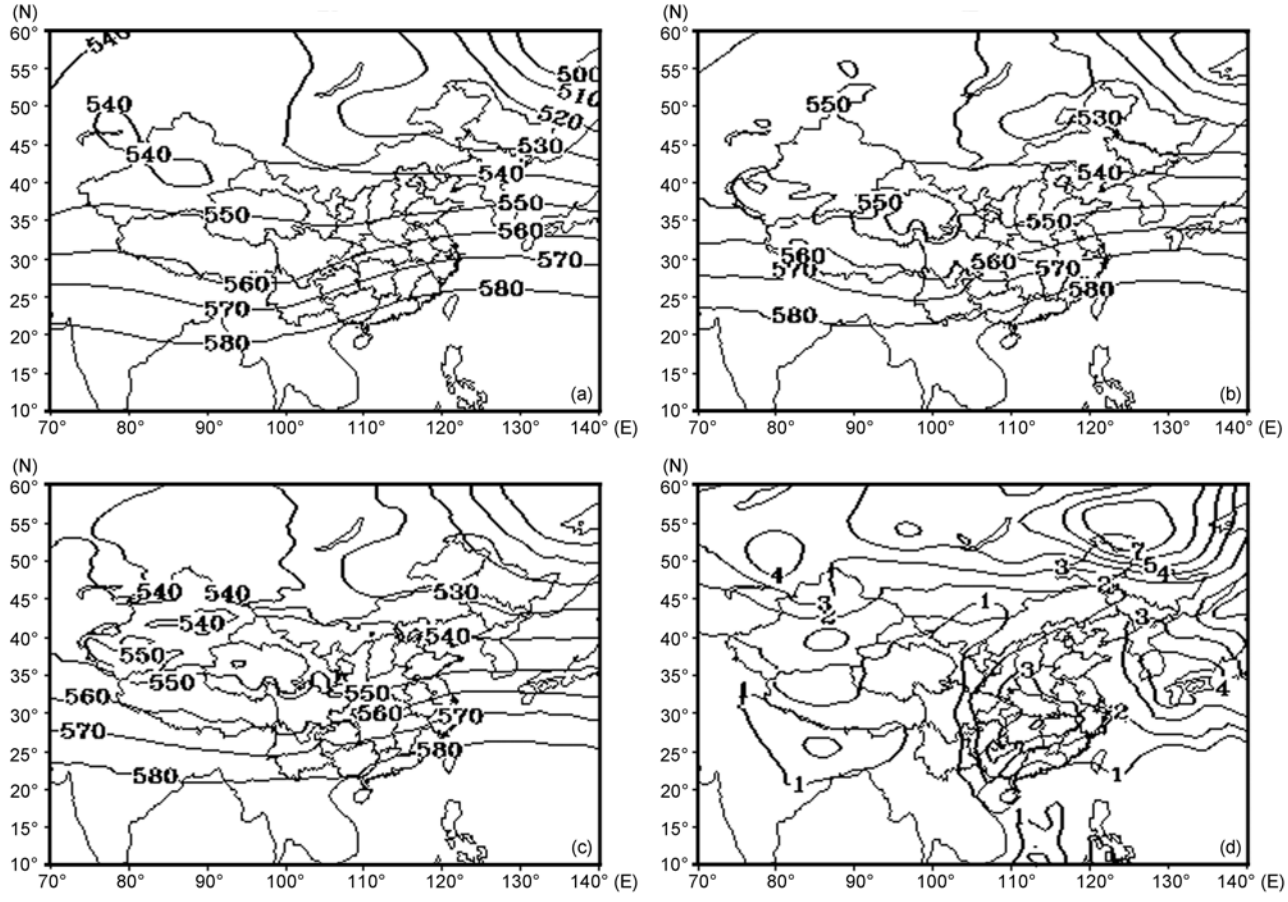

Figure 2 Geo-potential height fields comparison of 500 hPa. (a) ECMWF observed on 06 UTC 28 January 2008; (b) initialization without ATOVS assimilation; (c) initialization with ATOVS assimilation; (d) the difference with and without ATOVS assimilation.

with actual observation data. Observations were sampled at 00 and 12 (GMT), so these four simulated elements also were sampled at 00 and 12 (GMT), and time series data were compared during 10–30 Jan 2008, when the Frost Disaster was most severe.

Figure 3 provides the following results: 1) For temperature, the simulations without and with ATOVS assimilation are both in good agreement with the observations, but with slightly better simulation with ATOVS assimilation. 2) For geo-potential height, the evolution with and without ATOVS assimilation is in accordance with the measurements, but the modeled Geo-potential height after assimilation shows better agreement with the observation than without assimilation. 3) For humidity, the evolution is in accordance with the measurements, with relatively larger absolute error, but with slightly better simulation after assimilation than without assimilation. 4) For the wind vector field, the wind fields without and with ATOVS assimilation agree with each other, but with some improvement after assimilation.

Figure 3 also indicates that there were five decreasing temperature processes, having occurred on January 12, 16, 19, 25 and 28 respectively. The geo-potential height takes on the reverse phase compared to the temperature. The humidity changes greatly with time, which correlates positively with temperature changes, with 0.532 of correlation coefficient at 90% confidence level. The daytime temperature during days 19–24 is high and is stably maintained, while humidity fluctuates greatly between day and night. The RMSE (Root Mean Square Errors) and relative error showed that the simulation with ATOVS assimilation (i.e., after ATOVS assimilation) is improved, compared to that without assimilation (i.e., before assimilation, shorten as before hereinafter). Geo-potential height at 500 hPa, had a RMSE of 4.723 and 2.690 before ATOVS assimilation and after, with relative error of 0.078% and 0.043% before and after. Temperature at 500 hPa had a RMSE of 1.325 and 1.047 K before and after, with relative error of 0.036% and 0.029% before and after. Absolute humidity at 700 hPa, had a RMSE of 1.433×10^{-3} and 1.165×10^{-3} kg/kg before and after, with relative error of 17.568% and 14.591% before and after.

Comparison of results with and without ATOVS assimilation for the 500 hPa Geo-potential height with ECMWF analysis, four meteorological elements with observation and the RMSE scores indicate that simulation incorporating ATOVS improved the results, showing the practicability and reliability of the proposed regional ATOVS data assimilation scheme.

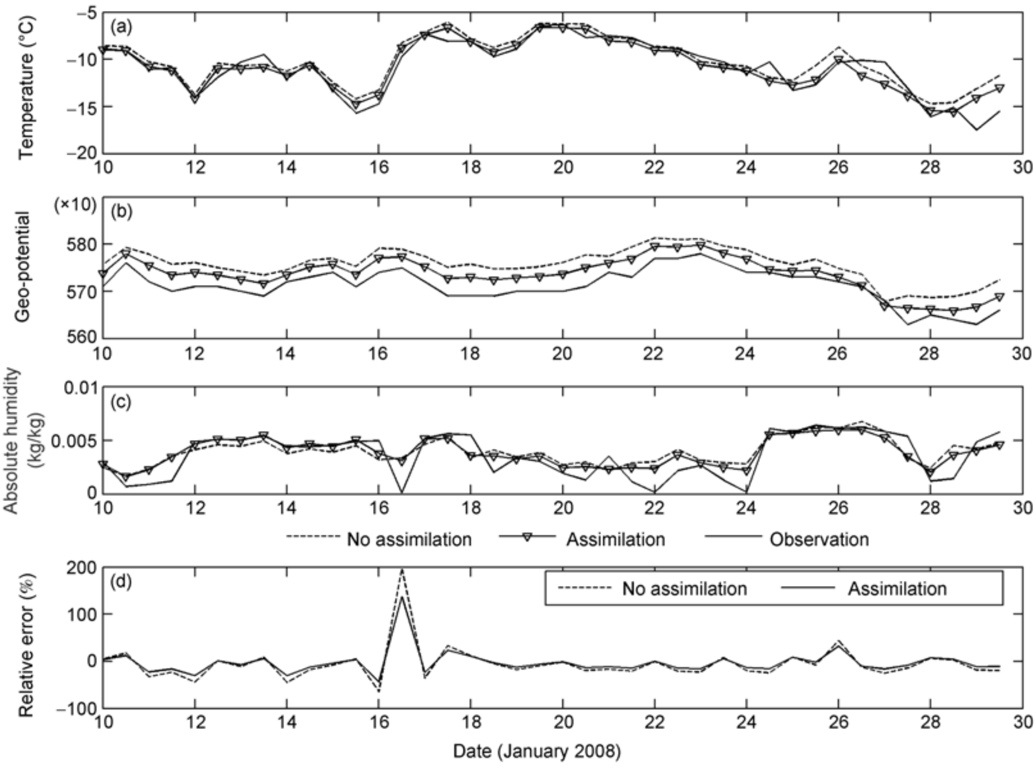

Figure 3 Comparison of observation and model results without and with ATOVS assimilation at Guizhou Station during January 10–30 of 2008 for air temperature (a), geo-potential (b), absolute humidity (c) and wind vector (d).

2 Calculation and validation of snow depth and snow water equivalent estimates based on ATOVS assimilation

2.1 Calculation of snow depth and snow water equivalent based on ATOVS assimilation

In snow disaster monitoring, snow depth is among the most important parameters, but it is currently difficult to derive from remotely sensed data. Therefore, the WRF system was adopted to calculate and forecast snow information based on the NOAH land surface sub-model, which can accurately simulate the snow processes of snowfall, sublimation and thawing, and the snow-soil thermal interchange. With the proposed scheme, snow depth and equivalent water can be calculated using the following procedures [29].

When the air temperature near the land surface is below 0°C, rain was converted into snow. The conversion from snow water equivalent to snow depth uses the formula $D_{\mathrm{snow}}=W_{\mathrm{snow}}/\rho_{\mathrm{snow}}$ (where W_{snow} and ρ_{snow} are snow equivalent water and snow density, respectively). These are added onto the original surface snow to give the primary estimation of snow depth. Snow evaporation/sublimation and thawing are computed using iterative procedures:

1) Calculate the potential evaporation based on first initialization of snow depth by $E_p=\rho_0 C_{\mathrm{h}}\left|V\right|[q_{\mathrm{s}}(T_{\mathrm{s}})-q_{\mathrm{a}}]$. Given the heat exchange, G, at the snow-atmosphere interface, potential evaporation, E_p, can be calculated by solving the surface energy balance equation:

$$\begin{aligned}&\rho_0 L C_{\mathrm{h}}\left|V\right|[q_{\mathrm{s}}(T_{\mathrm{s}})-q_{\mathrm{a}}]\\&=(1-\alpha)S^{\downarrow}+L^{\downarrow}-\sigma T_s^4-G-\rho_0 C_{\mathrm{p}} C_{\mathrm{h}}\left|V\right|(T_{\mathrm{s}}-T_{\mathrm{a}}),\end{aligned}\quad (1)$$

where ρ_0 is air density, L latent heat coefficient, C_{h} water vapor drag coefficient, C_{p} the thermal capacity of the air, T_s surface skin temperature (surface snow temperature at the time of the previous iterative step), and other near surface parameters in the model, such as wind speed ($|V|$), air temperature (T_{a}), and relative humidity (q_{a}). The expression on the left-hand side of the equation represents the latent heat flux. The five terms on the right-hand side of equation stand respectively for downward short- and long-wave surface radiation, upward long-wave radiation, the sensible and latent heat fluxes at the snow-soil interface. Given the snow depth, the heat flux at the snow-soil interface is obtained by the formula $G=K_{\mathrm{snow}}(T_{\mathrm{s}}-T_{\mathrm{soil}})/D_{\mathrm{snow}}$, where, T_{soil} is the soil temperature at the first layer, K_{snow} is the thermal diffusivity for snow. K_{snow} is set as 0.35 Wm/K.

2) Next compute the snow evaporation/sublimation E from the above estimated E_p. If $D_{\mathrm{snow}}\geqslant E_p\delta t$, E equals E_p; if $D_{\mathrm{snow}}<E_p\delta t$, E is estimated by $E=D_{\mathrm{snow}}/\delta t$, where δt is time step to invoke the land surface sub-model.

3) Finally, simulate the snow melting process, given the snow evaporation/sublimation E. If T_{s} is below 0, snow will not melt and if $T_{\mathrm{s}}>0$, evaporation/sublimation and melting will occur simultaneously. The snow melting process is derived iteratively by eq. (2):

$$\begin{aligned}&(1-\alpha)S^{\downarrow}+L^{\downarrow}-\sigma T_{\mathrm{s}}^4\\&=G+\rho_0 C_{\mathrm{p}} C_{\mathrm{h}}\left|V\right|(T_{\mathrm{s}}-T_{\mathrm{a}})+Q,\end{aligned}\quad (2)$$

where Q is the potential evaporation. To retrieve accurate snow melting parameters and the accumulated snow depth, the estimation process is iterated in three steps. First, Q (potential evaporation) is assumed to equal LE (actual evaporation/sublimation), and the effective surface skin T_{s} is iteratively estimated with eq. (2). Next, with the newly estimated T_{s} and the assumption that potential evaporation equals the sum of actual evaporation/sublimation and thawing ($Q=LE+L_i h_m$), eq. (2) can further be used to iteratively compute the thawing snow amount (h_m). Finally, if the estimated thawing snow amount is larger than the residual snow h'_m (defined as the residual land surface snow with evaporated/sublimated components deducted), then the residual snow will thaw completely and the land surface snow depth is 0. However, if h_m is smaller than h'_m, T_{s} is iteratively computed with eq. (2) with the assumption of $Q=LE+L_i h'_m$ (where L_i is the latent heat coefficient in terms of snow depth). The heat exchange G at snow-soil interfaces then can be estimated with the updated T_{s}, which is further used to calculate the final land surface snow depth, D_{snow}. In addition, snow water equivalent can be computed using the formula $D_{\mathrm{snow}}=W_{\mathrm{snow}}/\rho_{\mathrm{snow}}$. It should be noted that snow density might vary spatially across the extensive China snow cover region, which influences the relation of snow depth and snow equivalent water. This aspect of snow density difference is not explored in this study.

2.2 Validation of the modeled snow depth based on ATOVS assimilation

WRF snow depth results both with and without ATOVS assimilation (during 2008.1.18–2008.1.30) were compared with ground observations at six typical ground stations as shown in Figure 4 (i.e., Yaoxian of Shanxi Province, Lushan of Jiangxi, Nanyue and Anhua of Hunan, Wuhan of Hubei, and Chuzhou of Anhui). The WRF modeled results with or without ATOVS assimilation both underestimated actual land surface snow depth, although the ATOVS assimilation reduced this bias to a degree, especially during some time periods.

The temporal consistency of model results with observed snow depth was examined with six typical stations of snow cover in Figure 4, whereas Figure 5 provides a spatial consistency validation with 50 stations (randomly selected from 320 snow observation stations). In Figure 5, the development trend and process of NOAH-modeled snow depth agreed well with those from ground observations, which indicated that the WRF-coupled land surface model of

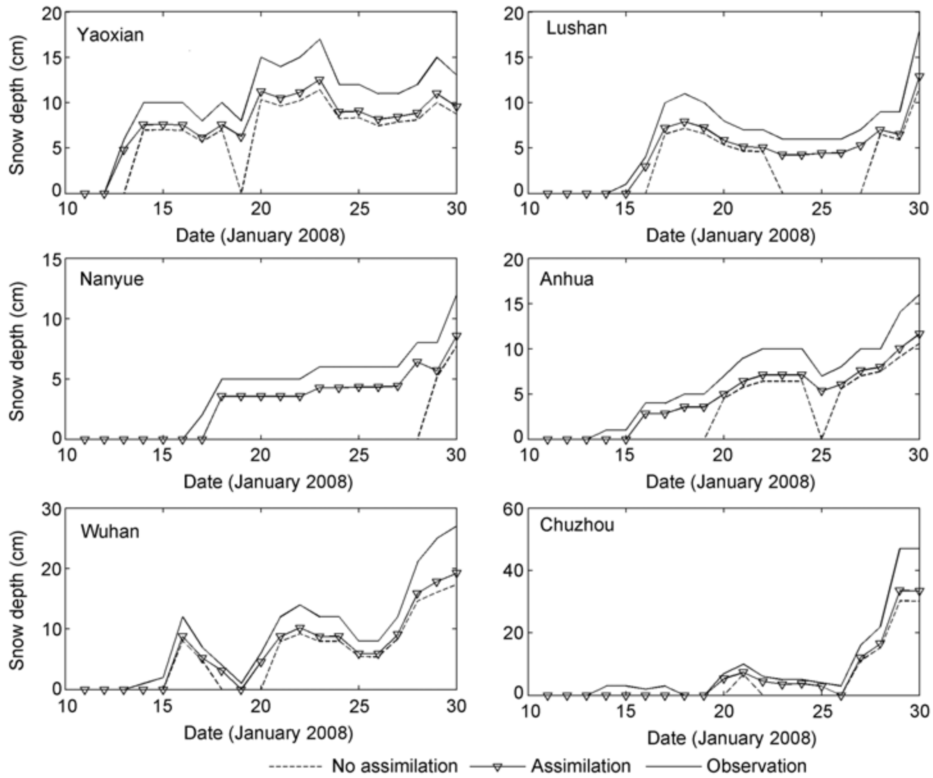

Figure 4 Snow depth comparisons of ground observations and WRF results with/without ATOVS assimilation. Six stations, on 10–30 January, 2008.

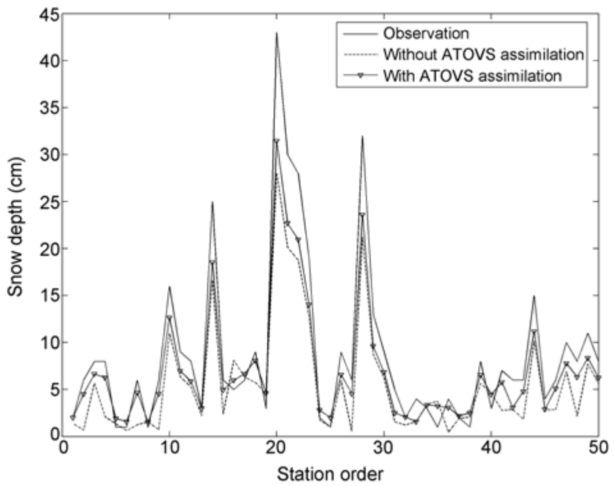

Figure 5 Snow depth comparison of ground observations and WRF results with/without assimilation. 50 stations, on 28 January, 2008.

NOAH could depict and model the snow processes in southern China during the 2008 Snowstorm. Both Figures 4 and 5 indicated the improvement achieved by ATOVS assimilation on the accuracy of WRF modeling results. The "underestimation" of the WRF may lie in the relatively coarse model spatial resolution of 30 km, as it is inconsistent in the spatial scale to validate modeled results of 30 km × 30 km region with the observation of a single ground point. In addition, systematic error of the WRF model may also lead to the "underestimation" since the result is biased whether ATOVS was assimilated (with RMSE of 4.819 cm) or not (with RMSE of 3.087 cm).

In summary, the above analyses of spatial and temporal consistencies between WRF results and observed snow depth indicate that although the coupled ATOVS assimilation is unable to completely remove the underestimation of the model results, it effectively depicts the development processes and snow depth trend, albeit with limited accuracy. This promises to be a practical and useful scheme for snow monitoring and analysis.

3 Monitoring the 2008 Snowstorm in South China

The regional ATOVS assimilation-based monitoring scheme for snowstorms described in the previous section can provide accurate and reliable information about snow depth and distribution, which has enabled us to analyze the spatial-temporal development processes of the 2008 Snowstorm in South China.

In general, snow cover characteristics in China vary distinctly with the region, so it is helpful to explore snow balance on the basis of snow cover zones for addressing spatial distribution characteristics of this snowstorm. The snow zone in the study takes into account both the conventional

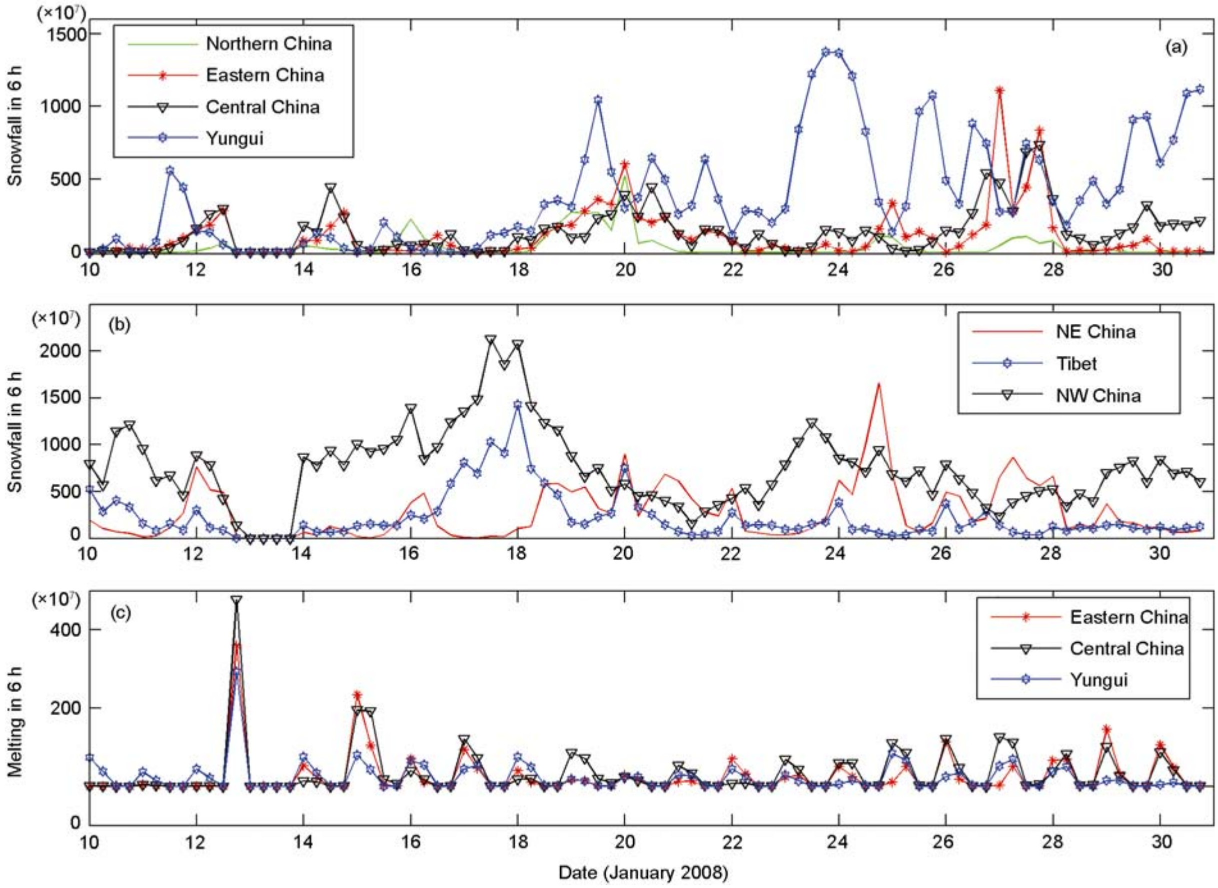

Figure 6 ATOVS assimilation-based modeling results of snowfall ((a), (b)) and thawing (c). Unit: 1×10^7 m^3.

district-based scheme (i.e., eight regions, Northwest, Northeast, North China, Central China, East China, South China, Yungui Plateau, and Tibetan Region) and the snow-related characteristics in geomorphology and climatology. Differing from the traditional scheme, the new zone divides the eastern, central, and western parts of Inner Mongolia respectively into the regions of Northeast, North China, and Northwest, and adjusts the Western Sichuan Plateau into the Tibetan Region, to make each snow region as geomorphologically and climatologically homogeneous as possible. The proposed snow forecast scheme can model snow depth variations of the land surface for certain periods (e.g., 00–06 Z), which can produce the variation of regional total snow volume by integrating depth with area information. Figure 6 shows the modeled snow fall (a, b) and thawing (c) every 6 hours during 10 to 30 January, 2008, where the horizontal/vertical axes were time and snow volume variation every 6 hours (unit: 1×10^7 m^3, referred as Unit later). Figure 6(a) indicates that the regions of Yungui, Central China, and East China, where it rarely snows heavily, experienced an obvious snowstorm process during this period. On 24 January, 2008, Yungui Region had a snow volume of about 1500 Unit, while the volume reached around the 1000 Unit level in the above three regions the same day. As the three regions are geographically located towards the east, this snow process showed a clear temporal sequence in its path, which agreed with those of related atmospheric processes. Figure 6(b) shows that the regions of Northwest and Tibetan Plateau had heavy snow from 17 to 18 January 2008. Though the snowstorm mainly took place in South China, the traditional snow cover regions (i.e., Northwest and Northeast China) experienced even more heavy snowfall during this period due to their higher latitude cold climates. Figure 6c shows the clear snow thawing processes on 13 and 15 January, 2008, (especially on 13 January, with a thawing volume of over 400 Units), which agreed with meteorological conditions of that time.

Based on meteorological observations, 10 January through 2 February 2008 saw four series of spatially extensive snow and freezing weather events in South China. The regions of Anhui, Jiangsu, Hunan, southeastern Henan, northern Jiangxi, and northern Zhejiang had heavy snow and even snowstorms in some regions. In the regions further south, i.e., eastern Hubei, Guizhou, southern Anhui, and the region south to the Yangtze River, freezing rain and freezing weather prevailed during that period. Among the four snow and freezing weather events, those of January 25–29 (Storm C), and January 31–February 2 (Storm D) were

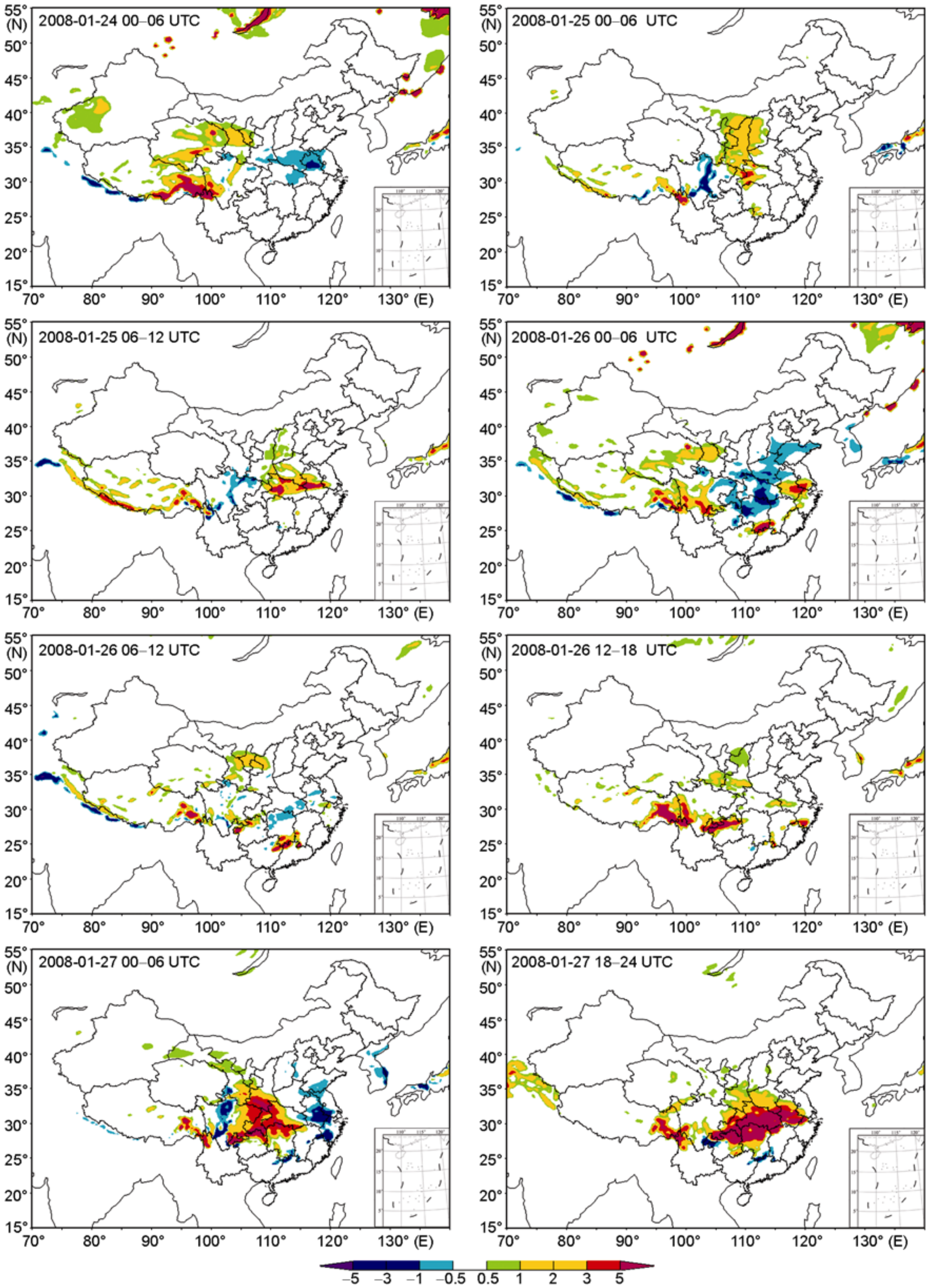
2008-01-24 00–06 UTC
2008-01-25 00–06 UTC
2008-01-25 06–12 UTC
2008-01-26 00–06 UTC
2008-01-26 06–12 UTC
2008-01-26 12–18 UTC
2008-01-27 00–06 UTC
2008-01-27 18–24 UTC
55° (N)
50°
45°
40°
35°
30°
25°
20°
15°
70°
80°
90°
100°
110°
120°
130° (E)
−5 −3 −1 −0.5 0.5 1 2 3 5

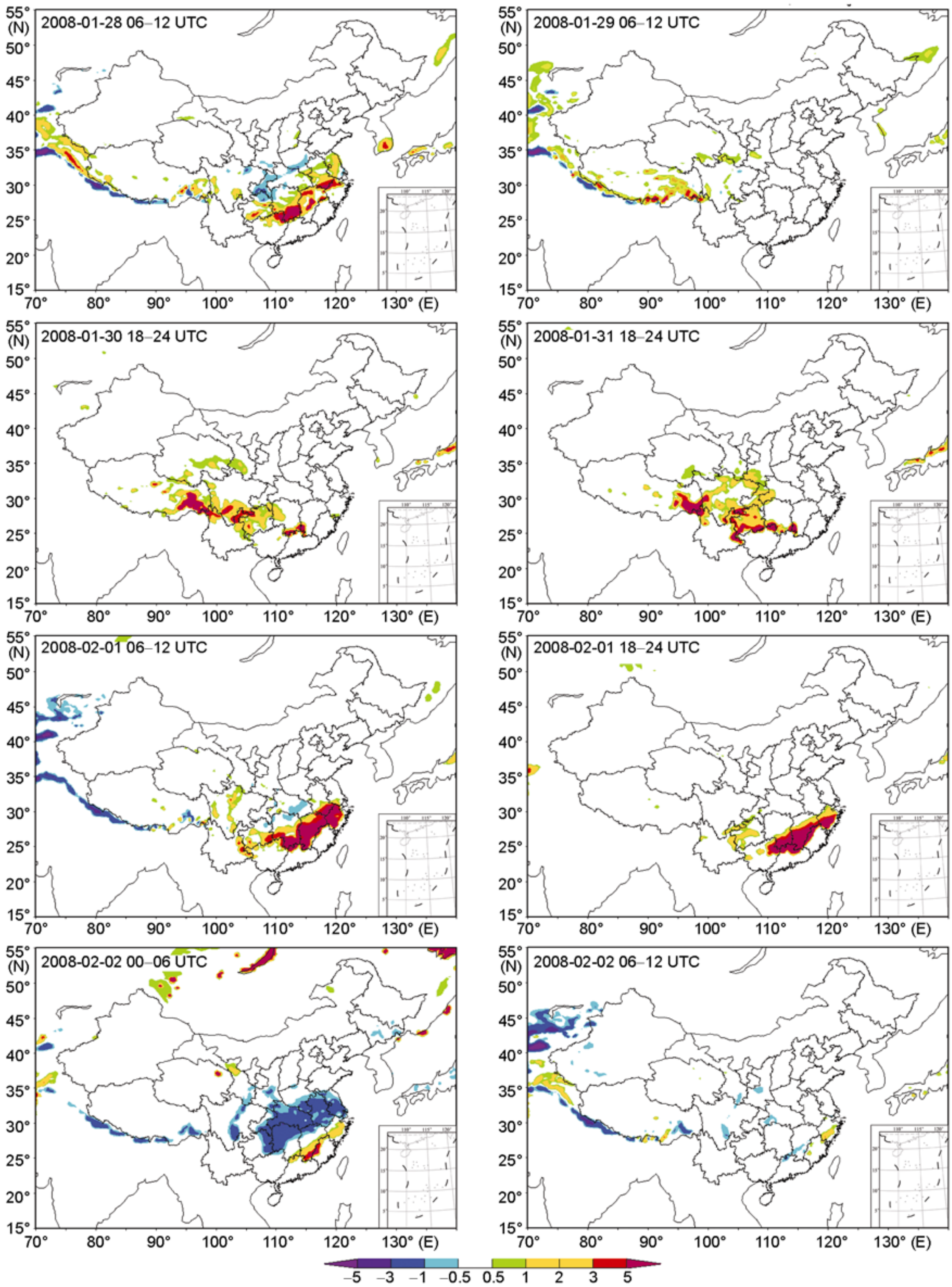

Figure 7 Spatial-temporal development of snow processes based on ATOVS assimilation. January 24–February 2, 2008. Snow water equivalent, in kg/m^2.

more heavy. Figure 7 shows the variation in simulated snow water equivalent (in kg/m^2) based on ATOVS assimilation every 6 hours during January 24 to February 2 of 2008. Figure 7 ignores those periods with little variation in snow thawing and snow fall. The positive and negative values represent net snowfall increase and snow thawing during the 6-hour period under discussion, respectively. The spatial-temporal development of the two snow processes was presented in Figure 7. Temporally, two snow processes (Storms C and D) existed during January 25–29 and January

31 to February 2, during which the latter led to serious and extensive freezing and a snow disaster in South China (which agrees with related report [40]). Spatially, Storm C originated north of southern Gansu Province on January 24, and moved into Shanxi and Central China; on January 26, this storm basically was in the thawing stage, whereas on January 27, its region of influence continued to move eastwardly into Hubei, Anhui, and northern Guizhou provinces. Storm D mainly affected the eastern region south to the Yangtze River, i.e., Jiangxi, Zhejiang, Hunan, Guangxi, Guangdong, and Guizhou. The storm was characterized by high intensity and high rate of development, reaching a snow water equivalent maximum of over 5 kg/m^2 for a time. This storm ran southwardly down over Guangdong and Guangxi on February 1, and then began to thaw quickly on February 2. Generally, the temporal change in snow water equivalent every six hours corresponded closely with spatial movement patterns of related weather processes. The spatial-temporal distribution of snowfall in Figure 7 also agreed closely with the statistical results of Figure 6 for snowfall and thawing.

4 Discussion and conclusions

4.1 Discussion

During January of 2008, serious snow and freezing weather occurred in South China. NSMC adopted ATOVS and NCEP data to drive the 3D-Var assimilation-coupled WRF system to establish a monitoring scheme for this snowstorm. The monitoring scheme produced snow information at resolutions of 1 hour temporally and 30 km spatially. These results were further used to model snow development processes using equivalent water every 6 hours. The model's results provided timely and valuable information for decision making related to the snow disaster. However, the modeled snow depth underestimated actual ground observations, which may result from systematic errors in the scheme.

The snow monitoring scheme in this study was designed and implemented due to the urgent need for a snowstorm emergency service, so other sources of remotely sensed data or products were not considered in the scheme. Therefore, the suggested scheme requires further development and improvement with respect to these related issues to make snow event forecast information even more accurate. We recommend, firstly, that further use of satellite VIS/IR images and microwave imager data be explored as soon as possible. Secondly, the introduction of additional data sources requires further discussion and evaluation. The ATOVS data assimilated in the proposed scheme was acquired by the NOAA-18 satellite. Three similar atmospheric vertical sounders onboard China's new generation FY-3 meteorological satellite, i.e., its Infrared Atmospheric Sounder (IRAS), Microwave Temperature Sounder (MWTS) and Microwave Humidity Sounder (MWHS), promise a new and reliable data source for storm monitoring in China. Therefore, future work on scheme improvements and data source extension can provide timely snow information with even higher accuracy for decision making for future snowstorm emergencies.

4.2 Conclusions

This study analyzed the relationship between snowfall and satellite-observed brightness temperatures, and proposed an ATOVS assimilation-based scheme for snowstorm monitoring. Results were compared with ground observations to examine the forecasting improvements contributed by a coupled assimilation sub-model. Successfully modeling and analyzing the spatial-temporal processes of this snow and freezing weather demonstrated the practicability and reliability of the proposed scheme. Through theoretical analyses and case studies, the following conclusions can be drawn.

1) Comparison of atmospheric circulation and snow depth before and after ATVOS assimilation validated the practicability and reliability of the proposed snowstorm monitoring scheme.

2) The coupling of ATOVS assimilation can effectively model the development trends of weather-related elements, e.g., the RMSEs of the 500 hPa altitude field before and after assimilation were 4.723/2.690 m respectively; the RMSEs of the 500 hPa temperature field before and after assimilation were 1.325/1.047 K respectively; and the RMSEs of the 500 hPa absolute humidity fields before and after assimilation were $1.33\times410^{-3}/1.165\times10^{-3}$ kg/kg respectively.

3) Though both the modeled results before and after assimilation underestimated the actual snow depth, the ATOVS assimilation reduced the RMSE of snow depth from 4.816 cm to 3.087 cm, and the snow depth development processes modeled by the data assimilation-based system better agreed with ground observations. Thus, snow information can be used effectively to analyze the development mechanisms and spatial-temporal processes of regional snowstorms.

4) The proposed scheme provided near-real time and valuable snow information for the 2008 Snow Storm in South China, which not only supported decision-making during the snow disaster emergency but also successfully developed a new field for the application of regional ATOVS data.

This work was supported by National Natural Science Foundation of China (Grant Nos. 40705037 and 40801175), the Open Fund by Numerical Model Innovation Base of China Meteorological Administration (Agreement 2006-12), and the R & D Special Fund for Public Welfare Industry (Meteorology GYHY(QX)2007-6-9).

1 Long X, Cheng L S. Numerical modeling for the "95.1" snowstorm event and its development of mesoscale system (in Chinese). J Lanzhou Univ (Nat Sci Ed), 2001, 37: 141–148
2 Wang J Z, Ding Y H. Research of moist symmetric instability in a strong snowfall in North China (in Chinese). Acta Meteor Sin, 1995, 53: 451–460
3 Gao Y Z, Zhou H L, Cang Y Q, et al. Weather analysis and prediction technology of snowstorm in Heilongjiang Province. J Nat Disasters, 2007, 16: 25–30
4 Kang Z M, Luo J X, Guo W H. Causality analysis of snowstorm in Xizang Plateau in Autumn of 2005. Meteor Mon, 2007, 33: 60–67
5 Yang L M, Yang T, Jia L H, et al. Analyses of the climate characteristics and water vapor of heavy snow in Xinjiang Region (in Chinese). J Glaciol Geocryol, 2005, 27: 389–396
6 Yi M. Review on the 2008 snowstorm occurred in South China (in Chinese). http://www.zgjrwx.com/Article_Show.asp?ArticleID=2666, 2008
7 China Meteorological Administration. Rules about Ground Surface Meteorological Observation (in Chinese). Beijing: China Meteorological Press, 2003
8 Jaedicke C. Snow mass quantification and avalanche victim search by ground penetrating radar. Surv Geophys, 2003, 24: 431–445
9 Koskinen, J, Pulliainen, J, Hallikainen, M. Effect of Snow Wetness to C-Band Backscatter-A Modeling Approach, Report 41. Espoo: Laboratory of Space Technology, Helsinki University of Technology, 2000
10 Negi H S, Mishra V D, Singh K K, et al. Application of ground penetrating radar for snow, ice and glacier studies. In: International Symposium on Snow Monitoring and Avalanches, SASE Manali, 12–16 April 2004
11 Romanov P, Tarpley D. Estimation of snow depth over open prairie environments using GOES imager observations. Hydrol Proc, 2004, 18: 1073–1087
12 Fu H, Li S M, Huang Z, et al. Verification and analysis of mathematical model for retrieved snow depth based on MODIS data (in Chinese). Arid Land Geog, 2007, 30: 907–914
13 Chang A T, Foster J L, Hall D K. Microwave snow signatures (1.5 mm to 3 mm) over Alaska. Cold Reg Sci Tech, 1987, 13: 153–160
14 Tait A B. Estimation of snow water equivalent using passive microwave radiation data. Rem Sen Environ, 1998, 64: 286–291
15 Kelly R J, Chang A T, Tsang L, et al. A prototype AMSR-E global snow area and snow depth algorithm. IEEE Tran Geosci Rem Sen, 2003, 41: 1–13
16 Che T, Li X. Armstrong R L. Estimation of snow water equivalent from passive microwave remote sensing data (SSM/I) in Tibetan Plateau. In: Microwave Remote Sensing of the Atmosphere and Environment III. 2003
17 Che T, Li X. Retrieval of snow depth in China by passive microwave remote sensing data and its accuracy assessment (in Chinese). Rem Sen Tech App, 2004, 19: 301–306
18 Moore J T, Blakley P D. The role of frontogenetical forcing and conditional symmetric instability in the Midwest Snowstorm of 30–31 January 1982. Mon Weather Rev, 1988, 116: 2155–2171
19 Wang W, Cheng L S. Numerical study of transversal wave instability for the "96.1" snowstorm event (in Chinese). Q J Appl Meteor, 2000, 11: 392–399
20 Jones S C, Thorpe A J. The three-dimentional nature of 'symmetric' instability. Q J R Meteor Soc, 1992, 118: 227–258
21 Chi Z X, Hu Y W, Bai H. Analysis on Symmetric Instability of "2003.1" Snowstorm Event in Southeast Guizhou (in Chinese). Plateau Meteor, 2005, 24: 792–797
22 Liu J J, Cheng L S. Diagnosis of Heat and Moisture Budgets of a Case of Storm Snow over the Plateau during December of 1997 (in Chinese). Meteor Mon, 2002, 28: 70–76
23 Zhang H, Xue J, Zhu G, et al. Application of direct assimilation of ATOVS microwave radiances to typhoon track prediction. Adv Atmos Sci, 2004, 21: 283–290
24 Eyre J R, Kelly G A, McNally A P, et al. Assimilation of TOVS radiance information through one-dimensional variational analysis. Q J Roy Meteor Soc, 1993, 119: 1427–1463
25 English S J, Renshaw R J, Dibben P C, et al. A comparison of the impact of TOVS and ATOVS satellite sounding data on the accuracy of numerical weather forecasts. Q J Roy Meteorol Soc, 2000, 126: 2911–2931
26 Bonan G B. Land Surface Model (LSM Version 1.0) for Ecological, Hydrological, and Atmospheric Studies. Technical Descriptions and User Guide, Technical Note NCAR/TN-417+STR, 1996. 150
27 Dai Y, Zeng Q C. A land surface model (IAP94) for climate studies. Part I: Formulation and validation in off-line experiments. Adv Atmos Sci, 1997, 14: 433–460
28 Ran M N, Qu J H, Sha L, et al. NOAA/ATOVS data obtaining, processing and displaying based on DVB-S system (in Chinese). J App Meteor Sci, 2006, 17: 19–25
29 Chen F, Dudhia J. Coupling an advanced land surface-hydrology model with the Penn State-NCAR MM5 modeling system. Part I: Model implementation and sensitivity. Mon Wea Rev, 2001, 129: 569–585
30 Michalakes J, Dudhia J, Gill D, et al. Design of a next-generation regional weather research and forecast model. In: Towards Teracomputing. River Edge: World Scientific, 1999. 117–124
31 Klemp J, Skamarock W, Dudhia J. Conservative split-explicit time integration methods for the compressible nonhydrostatic equations: WRF Eulerian prototype model equations on height and mass coordinates. http://www.WRF-model.org/WRFadmin/publications.php, 2000
32 William C S, Joseph B K, Jimy D, et al. A Description of the Advanced Research WRF Version 3. NCAR Technical Note, 2008. 126
33 Barker D M, Bray J, Guo Y, et al. Status report on WRF-ARW's Variational Data Assimilation System (WRF-VAR). 7th WRF Users' Workshop, 2006
34 Barker D, Huang W, Guo Y R. A three-dimensional variational (3DVAR) data assimilation system for use with MM5. NCAR Tech Notes NCAR /TN 2453 + STR, 2003
35 Lorenc A C. Analysis methods for numerical weather prediction. Q J R Meteor Soc, 1986, 112: 1177–1194
36 Eyre J R. A fast radiative transfer model for satellite sounding systems. In: ECMWF Research Department Technical Memorandum, 1991. 176
37 Liu Z, Barker D M. Radiance assimilation in WRF-Var: Implementation and initial results. 7th WRF Users' Workshop, 2006
38 Harris B A, Kelly G. A satellite radiance bias correction scheme for radiance assimilation. Q J R Meteor Soc, 2001, 127: 1453–1468
39 Eyre J R. A bias correction scheme for simulated TOVS brightness temperatures. In: Technical Memorandum, ECMWF, 1992. 28
40 Zheng G G. China is unprecedentedly experiencing a low temperature, heavy snowstorm and frost disasters (in Chinese). http://www.nmc.gov.cn/news/109879.html, 2008